COMMENTS ON PLASMA PHYSICS AND CONTROLLED FUSION

A Journal of Critical Discussion of the Current Literature

BURTON D. FRIED, *Co-ordinator*

A bimonthly journal devoted to critical commentaries on significant current developments appearing in scientific literature featuring columns in the fields of plasma physics and controlled fusion by a panel of eminent contributors.

COMMENTS ON MODERN PHYSICS

Part A: **Comments on Nuclear and Particle Physics**
Part B: **Comments on Solid State Physics**
Part C: **Comments on Astrophysics**
Part D: **Comments on Atomic and Molecular Physics**
Part E: **Comments on Plasma Physics and Controlled Fusion**

ANNUAL SUBSCRIPTION RATES (all subscriptions must be prepaid)

Individuals, who warrant that the journal is for their own use and order direct from the publisher postpaid

	EACH PART: 6 issues
Great Britain:	£8·50
U.S. and elsewhere:	\$21·00/£14·00

Libraries, research institutions and others, postpaid

Great Britain:	£23·00
U.S. and elsewhere:	\$47·00/£31·50

Subscriptions and changes of address should be sent to Gordon and Breach, Science Publishers, Inc., One Park Avenue, New York, N.Y. 10016 *or to* Gordon and Breach, Science Publishers Ltd., 42 William IV Street, London W.C.2.

APRIL 1977 issue.

Second-class postage paid in New York, N.Y. Mailed in the U.S.A. by Expediters of the Printed Word Ltd., 527 Madison Avenue, New York, N.Y. 10022, U.S.A.

Printed in England by The Press at Coombelands Ltd., Addlestone, Surrey.

Dynamic Stabilization of the Imploding-Shell Rayleigh–Taylor Instability

A method for dynamic stabilization of the Rayleigh–Taylor (R–T) instability on the surface of an imploding fusion pellet is discussed. The driving laser beams are modulated in intensity so the ablation layer is subject to a rapidly and strongly oscillating acceleration. A substantial band of the Rayleigh–Taylor instability spectrum can be stabilized by this oscillation even though the time average acceleration vector lies in the destabilizing direction. By adjusting the frequency, structure, and amplitude of the modulation, the band of dynamically stabilized modes can be made to include the most unstable and dangerous modes, Thus considerably higher aspect ratio shells (i.e., thinner shells) could implode successfully than had been previously considered stable enough.[1] Both theory and numerical simulations support this conclusion for the case of laser-driven pellet implosions. Similar modulation via transverse beam oscillations or parallel bunching should also work to stabilize the most dangerous surface Rayleigh–Taylor modes in relativistic electron-, ion- and heavy ion-pellet fusion schemes.

Common schemes for producing thermonuclear fusion by imploding a solid sphere or hollow shell containing D–T fuel rely on the symmetry of the implosion to achieve a strong enough compression to initiate the thermonuclear burn process. The prevalent schemes suggested to date (laser beams, electron beams, light or heavy ion beams incident on the surface of a layered pellet) all involve deposition of energy in a thin ablation layer at the surface of the pellet. This energy rapidly heats the dense shell material causing a high pressure region. This pressure maximum accelerates the bulk of the shell inward and conserves momentum by accelerating a low density blow-off plasma outward. Figure 1 shows the density, temperature, and pressure profiles at the outside of a D–T shell being accelerated by a thermal conduction ablation layer. These profiles are presented exactly as computed by the FAST2D computer code used in the simulations described later. The

Comments Plasma Phys. Cont. Fusion 1977, Vol. 3, No. 1, pp. 1–13

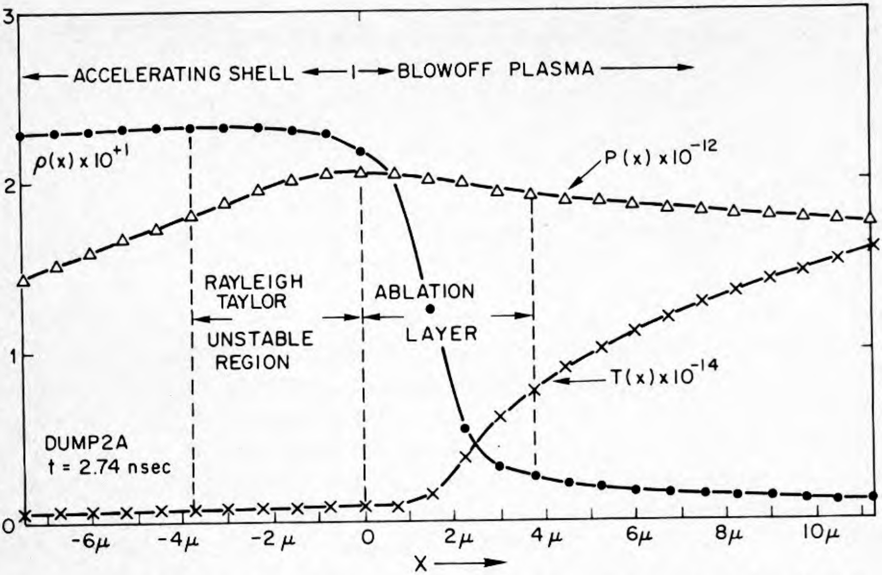

FIGURE 1. Density (●), pressure (△) and temperature (×) profiles for a thermal conductivity ablation layer. Data are taken from a two-dimensional simulation using FAST2D. The temperature at the critical layer was taken to be 3×10^{14} cm^2/s^2 (about 500 eV). The Rayleigh-Taylor modes are potentially unstable where density and temperature gradients are opposed.

laser deposits its energy at the critical layer (off the right-hand side of the figure). Since the $x = 0$ position coincides with the peak pressure point, the blow-off lies to the right ($x > 0$) and the accelerating shell lies to the left ($x < 0$). The ablation layer proper extends about 3 or 4 μm from the separation point $x = 0$ out into the blow-off and results from the strong nonlinear dependence of the thermal conductivity on temperature.

Since the relatively low density ablation layer is accelerating the higher density shell, the system is unstable to the Rayleigh–Taylor modes which can grow when the acceleration lies parallel to the density gradient. The detailed behavior of the instability is complicated by a host of important physical effects so not even the linear problem has been solved adequately. Computer codes such as LASNEX[2] and FAST2D[3] have been used to study some of the properties of the Rayleigh–Taylor modes via numerical simulation and some of the linear properties of the R-T modes have been uncovered analytically. Unfortunately an accurate dispersion relation including finite sound speed, ablation layer gradients, convection and finite thermal conductivity still does not exist to describe the growth of these modes. Furthermore, the nonlinear growth and turbulence properties are almost entirely a mystery.

The nonlinear properties of the R-T modes will be the subject of future research. For now I concentrate on the two main linear results of the Rayleigh-Taylor analysis obtained by using the simulation codes.

1. The long wavelength R-T modes appear to follow the incompressible $\gamma \sim (ka)^{1/2}$ law well beyond the wavelengths where sonic communication across a wavelength takes longer than a growth time.
2. There is a cutoff beyond which shorter wavelengths are stabilized by the finite thickness of the ablation layer and/or dissipative terms. Longer wavelengths grow.

The fully nonlinear equations being solved in the FAST2D model[3] are:

$$\frac{\partial \rho}{\partial t} = -\frac{\partial}{\partial x}(\rho V_x) - \frac{\partial}{\partial y}(\rho V_y) \tag{1}$$

$$\frac{\partial(\rho V_x)}{\partial t} = -\frac{\partial}{\partial x}(P + \rho V_x V_x) - \frac{\partial}{\partial y}(\rho V_y V_x) \tag{2}$$

$$\frac{\partial(\rho V_y)}{\partial t} = -\frac{\partial}{\partial x}(\rho V_x V_y) - \frac{\partial}{\partial y}(P + \rho V_y V_y) \tag{3}$$

$$\frac{\partial E}{\partial t} = -\frac{\partial}{\partial x}\left[E V_x + P V_x - K_0 T^{\frac{5}{2}} \frac{\partial T}{\partial x}\right] - \frac{\partial}{\partial y}\left[E V_y + P V_y - K_0 T^{\frac{5}{2}} \frac{\partial T}{\partial y}\right] \tag{4}$$

where $K_0 \sim 10^{-33}$ is used for D–T and where the temperature has kinetic units of $\mathrm{cm}^2/\mathrm{s}^2$. That is, $P \equiv \rho T$ and $E = P/(\gamma - 1) + \frac{1}{2}\rho V^2$. The value of γ is taken to be 5/3 throughout the material and the $T^{5/2}$ plasma thermal conduction is used in the shell as well.

The calculations used later to demonstrate dynamic stabilization were performed with typical values $0.5\mu \leqslant \delta x \leqslant 1.0\mu \leqslant \delta y < 5\mu$ and with 0.5 ps $< \delta t <$ 2.5 ps. The sound and flow speeds determine the timestep by the usual Courant conditions and the sliding rezone capability of the FCT algorithms is used to perform the calculation in an accelerating frame of reference which keeps the dense shell material centered in the computation region throughout the run.

The numerical results to date are consistent with a very simple phenomenological dispersion relation for the growth of the Rayleigh-Taylor modes,

$$\gamma^2 = \frac{ka}{1 + k/k_\rho} - \frac{4k^2 a}{3k_\rho}. \tag{5}$$

This has the desired cutoff at $k_c = k_\rho/2$ and also has $\gamma \sim (ka)^{1/2}$ for long wavelengths, supported by simulation. In Eq. (5) the acceleration of the shell is a, k_ρ is the inverse scale length for the high density half of the ablation layer, and $k = 2\pi/\lambda$ is the wave number of the Rayleigh-Taylor modes in the y-direction along the shell. Defining $\varepsilon \equiv k/k_\rho$ gives

$$\gamma^2 = k_\rho a\left[\frac{\varepsilon}{1+\varepsilon} - \frac{4\varepsilon^2}{3}\right] \tag{6}$$

where the shortest linearly unstable mode has $\lambda = 4\pi/k_\rho$. Maximum growth occurs at $\varepsilon \sim \frac{1}{4}$ and the value of the growth rate maximum is $\gamma_{\max} \sim (k_\rho a)^{1/2}/3$.

To study the effects of modulating the laser beam numerically, the plasma temperature at the critical surface was varied according to a prescribed functional form, constant plus a sinusoidal oscillation. To study the same phenomenon analytically in an approximate but illuminating manner, the dispersion relation Eq. (5) was converted to a second-order ordinary differential equation for the perturbation mode amplitude. Then the acceleration term is varied parametrically. This equation,

$$\frac{\partial^2 A}{\partial t^2} = \left[\frac{k_\rho a(t)\varepsilon}{1+\varepsilon} - \frac{4\varepsilon^2 k_\rho}{3}\langle a(t)\rangle\right]A, \tag{7}$$

like the dispersion relation on which it is based, has only a phenomenological/numerical basis because the linear, time-constant-coefficient problem has not been solved satisfactorily to date. The acceleration in the cutoff term is taken as a time average although some additional stabilization might result from including in the theory the oscillating thickness of the ablation layer itself.

Let $a(t) = a_0 + a_1 \cos \omega t$ where a_0 is the time average part and a_1 is the amplitude of the oscillating acceleration. The ordinary differential equation (7) becomes

$$\frac{\partial^2 A}{\partial t^2} = \left[\frac{\varepsilon}{1+\varepsilon}(k_\rho a_0 + k_\rho a_1 \cos \omega t) - \frac{4\varepsilon^2 k_\rho}{3} a_0\right]A \tag{8}$$

where ω is the frequency of the modulation. The time dependence is assumed here to be simple, periodic, and sinusoidal. There is no reason to assume that the sinusoidal modulation is optimal but at least it is analytically tractable. Putting Eq. (8) in the form of the canonical Mathieu Equation[4] as treated in Morse and Feshbach (see Figure 2) requires $2\phi = \omega t$ and gives

$$\frac{\partial^2 A}{\partial \phi^2} = \left[\frac{4k_\rho a_1 \varepsilon}{\omega^2(1+\varepsilon)}\cos 2\phi - \frac{4k_\rho \varepsilon a_0}{\omega^2(1+\varepsilon)} - \frac{16k_\rho \varepsilon^2}{3\omega^2} a_0\right]A. \tag{9}$$

We identify coefficients as follows

$$\frac{h^2}{2} = \frac{4k_\rho a_1}{\omega^2}\frac{\varepsilon}{1+\varepsilon}$$

and

$$b = \left[\frac{4k_\rho a_1}{\omega^2}\frac{\varepsilon}{1+\varepsilon} - \frac{4k_\rho a_0}{\omega^2}\frac{\varepsilon}{1+\varepsilon} + \frac{16k_\rho \varepsilon^2}{3\omega^2}a_0\right]. \tag{10}$$

Let $f_1 \equiv \dfrac{4k_\rho a_1}{\omega^2}$ and $\delta \equiv a_0/a_1$. Then

$$\frac{h^2}{2} = \frac{f_1\varepsilon}{1+\varepsilon} \quad \text{and} \quad b = \frac{h^2}{2} - \frac{h^2}{2}\delta\left[1 - \frac{4\varepsilon}{3}(1+\varepsilon)\right] \tag{11}$$

are obtained as the appropriate non-dimensional Mathieu Equation coefficients. Here both a_0 and a_1 are positive constants.

With the values of h and b determinable from Eqs. (11) above, we turn to Figure 2 which shows the stability regions for solutions of Mathieu's

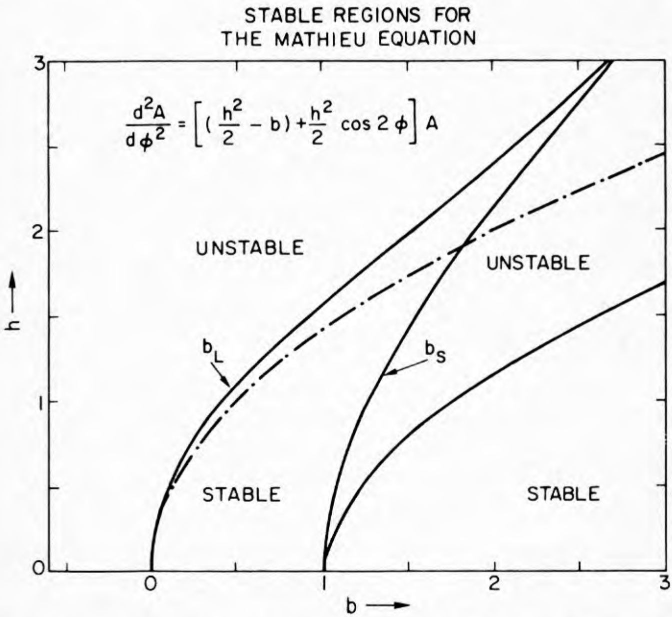

FIGURE 2. Stability diagram for the Mathieu Equation. The region of b–h parameter space between the curves labelled b_L and b_S is dynamically stabilized by the oscillatory modulation. The dashed curve is the locus of the Rayleigh-Taylor spectrum in the limit of large amplitude oscillations. The locus displaces to the left slightly as the average acceleration approaches the size of the oscillating component.

Equation. The regions of stability and instability are separated by the solid lines in the figure. We need consider only the upper half plane because the even power h^2 is determined from the physical parameters. Above and to the left of the line labelled b_L at least one of the two independent solutions of Eq. (9) grows without bound. Two stable bands are shown, one between the lines b_L and b_S and the other in the lower right-hand corner for large positive b. The first region is accessible by oscillating the laser intensity but the second is not because *b is generally less than $h^2/2$* by Eq. (11). This limit is shown as the dashed line in Figure 2. For finite values of δ the locus of (b, h) values as a function of ε from Eq. (11) is displaced to the left from the dashed line for finite wavelengths. Under such a displacement only a band of Rayleigh-Taylor modes is stabilized and we need to study the extent of this stable band.

The first stability boundary is given by

$$b_L \approx \frac{h^2}{2} - \frac{h^4}{32} + \frac{7h^8}{1024 \times 32} + \cdots \tag{12}$$

as determined from Abramowitz and Stegun.[4] From the same source the second stability boundary is found to be

$$b_S \approx 1 + \frac{h^2}{4} - \frac{h^4}{128} + \cdots \tag{13}$$

The subscripts L and S refer to the long and short wavelength limits of the first stable region respectively. We want to find the broadest band of stabilization that can be achieved given some control over ω and a_1 for the modulation. One needs to determine first the value of f_1 for which the linearly most unstable mode $\varepsilon \sim \frac{1}{4}$ lies right on the short wavelength stability boundary. We do this by setting $b(\varepsilon = \frac{1}{4}, h) = b_S(h)$ and solving for the value of h^2. The result is relatively simple for small δ (i.e., $a_0/a_1 < \frac{1}{4}$).

$$h_S \approx 4\left\{\left[\left(1 - \frac{7\delta^2}{6}\right) + \frac{1}{2}\right]^{\frac{1}{2}} - \left(1 - \frac{7\delta}{6}\right)\right\}^{\frac{1}{2}} \sim 2. \tag{14}$$

Using $h_S = 2$ in Eq. (11) allows us to determine

$$f_1 = \frac{4k_\rho a_1}{\omega^2} \sim 10 \tag{15}$$

as the required combination of k_ρ, a_1 and ω such that the linearly most unstable mode is just stabilized by the modulation. Perhaps f_1 can be increased beyond this limit even though a narrow band of short wavelength unstable modes might appear but $f_1 = 10$ is a simple, easy to remember criterion.

Given δ and f_1, we can solve for the long wavelength limit of the dynamically stabilized band by setting $b = b_L$ and solving for the value ε_L at which marginal dynamic stability occurs. We get

$$\frac{h^2}{2} - \frac{h^2}{2}\delta\left[1 - \frac{4\varepsilon_L}{3}(1 + \varepsilon_L)\right] = \frac{h^2}{2} - \frac{h^4}{32} + \cdots$$

which has the approximate solution

$$\varepsilon_L \sim \frac{8\delta}{f_1}\left[1 - \frac{8\delta}{f_1}\right]. \tag{16}$$

when $f_1 = 10$, the longest stable wavenumber is

$$\varepsilon_L \sim 0.8\delta\left[1 - \frac{8}{30}\delta\right] \sim \frac{4\delta}{5}. \tag{17}$$

The width of the stabilized band is therefore given by the simple formula

$$\varepsilon_L \equiv \frac{k_L}{k_\rho} \approx \frac{4a_0}{5a_1}. \tag{18}$$

Clearly the larger the ratio of a_1 to a_0, the longer the wavelengths that can be dynamically stabilized. In one of the computer calculations RUN 1G (see Figure 3) the ratio $\delta = a_0/a_1$ was measured to be of the order 0.2 to 0.1. It is not clear exactly what to use as a_1 because there are strong spatial gradients in the region prone to Rayleigh-Taylor instability. Thus $k_L \approx \frac{1}{9}k_\rho$ as an estimate. Since the ablation layer thickness k_ρ^{-1} lay in the range 1 to 2μm (also estimated by seeking the most unstable wavelength $\lambda_m \sim 13\mu$m and the cutoff wavelength $\lambda_c < 10\mu$m), the longest stable wavelength for that run could be expected to lie in the range 30μ to 70μm. In fact, the mode with $\lambda = 60\mu$m grew slowly.

To maximize the effectiveness of this dynamic stabilization one clearly wants to minimize ε_L in Eq. (17). This is accomplished by reducing δ and increasing f_1 subject to the constraint that short wavelengths 'uncovered' at large k by pulling the dynamic stabilization 'blanket' to small k (minimizing ε_L) do not fracture the shell. There is also another constraint on increasing f_1 which arises because a_1 and ω are really coupled. When ω is too small (to maximize f_1), the value of a_1 also decreases because the ablation layer and the Rayleigh-Taylor unstable region beneath can adjust rather quickly to changes in the driving pressure.

Further work is definitely required to pin down more accurately what the accessible regime of values of f_1 is. We turn now to the very important question of how this dynamic stabilization effect scales with size. Larger pellets with thicker shells implode more slowly so it is important to stabilize proportionately longer wavelengths. When the overall shell thickness ΔR is

increased, a_0 decreases as ΔR^{-1} since the average shell acceleration goes inversely as the total mass at a fixed ablation pressure. The oscillating acceleration a_1 is unaffected by the shell thickness so the ratio $\delta \equiv a_0/a_1$ also decreases as ΔR^{-1}. This has two advantages when scaling up to larger pellets. First, the long wavelength stable-to-unstable crossover point at $k_L \approx 8\delta k_\rho/f_1$ moves progressively toward longer wavelength (smaller ε) as δ approaches zero. This means that longer wavelengths can be stabilized by a given modulation frequency and amplitude in large pellets than in small pellets. Second, a smaller value of δ means that correspondingly lower modulation frequencies can be tolerated since $a_1 > a_0$ is easier to ensure in large pellets than in small.

The conclusion is that, by varying ω, the most unstable mode with wave number $k_m \sim \frac{1}{4}k_\rho$ can be moved right to the boundary of the stable region near $b \sim 1.8$, $h \sim 1.9$ (or beyond) to maximize the extent of the dynamically stabilized portion of the Rayleigh-Taylor spectrum. Furthermore, as has been seen in several complete numerical simulations, the region stabilized is quite broad enough to increase the workable aspect ratio of the imploding shell considerably.

Several sets of two-dimensional computer simulations have been performed to test dynamic stabilization in a realistic system which contains the finite sound speed/shock properties of the fluid involved and which also represents accurately the nonlinear thermal conductivity effects expected. The laser is assumed to be incident from the $x = x_{max}$ boundary of the system and deposits energy at the critical density $\rho \sim 0.004$ g/cm^3 in such a way that the temperature at the critical density is specified as a controlled time-dependent parameter. The location of the critical layer is allowed to change naturally with time.

Figure 3 summarizes the results of a set of calculations performed on a 40×40 finite difference grid. Three different runs were performed with differing laser intensity profiles. The reference run, labelled RUN 1C, began with a temperature at the critical layer of 1×10^{14} cm^2/s^2. This corresponds to about 175 eV. The temperature linearly increased to 2×10^{14} cm^2/s^2 in 0.5 ns and then was held constant at that level for the remainder of the run.

In this reference case without dynamic stabilization the linear growth rates for the modes near $\varepsilon \sim 0.25$ were determined roughly from the calculation and supported reasonably well the dispersion relation given in Eq. (5). The solid curve in Figure 3 shows the velocity of the shell as a function of time up to the point at which the shell buckled due to the Rayleigh-Taylor instability. There was no laser modulation in the reference calculation and the time of buckling was determined to be that time when the maximum perturbation of the ablation layer was $\pm 2\mu$m. This, of course, corresponds to a far smaller perturbation on the inside edge of the shell.

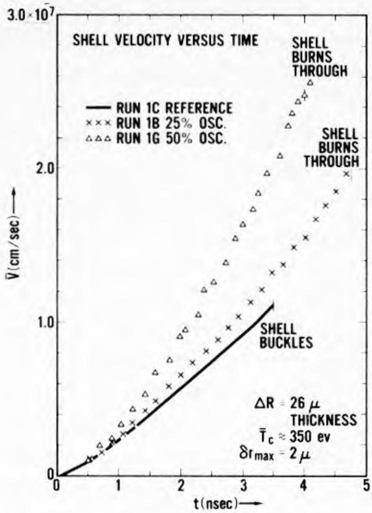

FIGURE 3. Comparison of shell velocity versus time trajectories for three calculations demonstrating dynamic stabilization of the laser shell Rayleigh-Taylor mode. With dynamic stabilization the shell does not buckle due to the Rayleigh-Taylor instability before the ablator material simply burns through.

The calculation labelled 1B in the figure was performed using the reference temperature profile plus a 25% oscillation of the laser intensity superimposed. The amplitude of the oscillation therefore was 5×10^{13} cm^2/s^2 and the oscillation frequency was taken to be three cycles per ns. The shell in RUN 1B accelerated somewhat faster than the reference case 1C because the extra energy deposited at the peak of the oscillation (because the thermal conductivity is nonlinear) exceeds the energy decrement in the trough. The shell also accelerates for a somewhat longer period of time, reaching a terminal velocity roughly twice the velocity attained in the reference case. The calculation was terminated, not when the shell buckled, but when the laser pulse burned through the accelerating ablator material. Thus the shell did not go Rayleigh-Taylor unstable; it simply became too thin.

RUN 1G, plotted as triangles in Figure 3, was performed with a 50% oscillation at 2.25 cycles/ns superimposed on the linear ramp plus constant temperature profile. The oscillating temperature at the critical layer was $\pm 10^{14}$ cm^2/s^2 and the acceleration is correspondingly faster than either the reference case 1C or the 25% oscillation case 1B. The shell again burns through rather than buckling. The velocity attained before burnthrough is now roughly 2.5×10^7 cm/s. More than six times the kinetic energy per particle has been translated to the shell in the dynamically stabilized

modulated case as opposed to the unstable reference case. The time of acceleration and burnthrough for the 50% modulation in RUN 1G is somewhat shorter than the 25% oscillation because the rate of ablation and hence the acceleration is somewhat larger.

To pursue dynamic stabilization further, runs with a thicker shell were clearly required and runs with $\delta y > \delta x$ were needed to study the effects of dynamic stabilization on longer wavelengths. Greater resolution was also called for to increase the breadth of the potentially unstable portion of the spectrum. A set of four calculations were performed on an 80×80 finite difference grid with a somewhat higher base temperature and with a shell thickness of $37 \mu m$ initially. The idea was to perform an entire reference calculation without modulation and then to restart that identical calculation in the middle when initial wave amplitudes had grown out of the early random noise and mode growth was beginning to occur in an organized linear manner. The modulated case was restarted with a 33% oscillation at two cycles/ns and the evolution of the same initial conditions with and without modulation were compared. The driving temperature ramped linearly up to 3×10^{14} cm^2/s^2 and then was held constant for the duration of the reference calculation. The amplitude of the oscillation added to this constant temperature was 1×10^{14} cm^2/s^2. Figure 1 shows the ablation layer structure for this 80×80 reference run.

After about 3 ns the mode structure was sufficiently well developed and yet the amplitudes were sufficiently small that the modulation could be started and the dynamic stabilization properties tested on a difficult case which had been allowed to grow unchecked for more than 3 ns. After the modulation had been established, the fastest growing Fourier harmonics of the ablation layer perturbation became essentially oscillatory and stopped growing. The perturbation was held to a couple tenths of a micron amplitude. In the reference calculation without dynamic stabilization, the shell became Rayleigh-Taylor unstable and broke at about 6 ns. The $2 \mu m$ perturbation limit was again used as a signature of shell breaking for the unmodulated reference case and the modulated case showed shell burnthrough rather than Rayleigh-Taylor buckling.

Two runs were then performed to study the long wavelength effects in this 80×80 system with the thicker $37 \mu m$ shell. These two runs used the same reference temperature profile but the critical layer temperature oscillation amplitude was increased to 50%. The period of the oscillation was reduced to 1 cycle/ns to maximize f_1 and hence to broaden the band of dynamic stabilization. The two runs were performed with $\delta y = 1.25 \mu m$ and $\delta y = 3.75 \mu m$ so the longest wavelength in the runs would be $100 \mu m$ and $300\ \mu m$, respectively.

Again the shell burned through rather than breaking due to Rayleigh-

Taylor instability. The shell attained a velocity of 3.5×10^7 cm/s and showed no serious buckling before burnthrough. In most cases the outer surface perturbation at burnthrough was at most a couple tenths of a micron, a good order of magnitude *below* the level used to signal Rayleigh-Taylor buckling in reference calculations such as shown in Figure 3. From the stability of the two runs we conclude that modes of at least 300μm wavelength along the shell are dynamically stabilized by modulating the laser intensity.

For these runs the speeds of 3×10^7 cm/s attained in 6 ns gives an average acceleration of $a_0 \sim 5 \times 10^{15}$ cm/s^2 for the run. The fluctuating component of the acceleration could also be estimated from the data as $a_1 \sim 1\text{–}2 \times 10^{16}$ cm/s^2. Inserting into Eq. (15), defining f_1 and using $k_\rho^{-1} \sim 1.5\mu$m and $\omega = 2\pi \times 10^9$ s^{-1}, gives $f_1 \sim 7\text{–}13$ which nicely brackets the theoretical target value of $f_1 \sim 10$.

In 6 ns at an average velocity of roughly 1.5×10^7 cm/s the shell travels 900μm. If the initial spherical shell were of order 1000μm in radius, this case would represent a (relatively) successful implosion of a 30:1 aspect ratio system.

The crucial question of how large the constant f_1 in Eq. (15) can be made and hence how broad a band of modes can be stabilized is only partially answered. In one of the early 40×40 calculations a frequency of 6 cycles/ns was tried and the shell went Rayleigh-Taylor unstable almost as if no modulation had been applied. A high frequency cutoff is expected because temperature variations at the critical layer cannot be felt at the ablation layer unless their period is longer than the heat diffusion time.

A 40×40 run was also performed with a modulation frequency of 1 cycle/ns but this proved to be too long on such a small system. In the troughs of the oscillation the shell tried to expand out of the computation region, a problem later rectified in the series of 80×80 calculations. For the typical parameters of interest here frequencies of $\sim$0.5 cycle/ns and slower have yet to be considered and may work best of all. Clearly, however, the period of the modulation cannot be longer than a few growth times. It may even be possible to leave short wavelength modes unstable to stabilize even longer modes. Certainly the range of interesting ω values spans about an order of magnitude.

Since the portion of the laser energy which gets deposited at the critical surface depends on a number of laser and fluid parameters and since the thermal conduction, which converts temperature at the critical layer to acceleration at the ablation layer, is highly nonlinear, one can only guess what the laser intensity profile would have to be in order for the acceleration to be sinusoidal as assumed in the theory. It is safe to guess that the numerical simulations performed to date are not yet optimum and, therefore, the stabilization conclusions presented are correspondingly conservative. What

also remains to be determined is the effect on dynamic stabilization of the host of non-ideal effects such as radiation, atomic physics, realistic equations of state, self-magnetic fields, and suprathermal particle effects which can also broaden the ablation layer and hence change the short wavelength cutoff.

Dynamic stabilization works in the laser-driven implosion because the shell must compress somewhat to transmit the acceleration from the ablation layer on the outside throughout the shell. Therefore an outward acceleration of necessity arises to relieve the shell compression when the laser intensity reaches a minimum. The fluid compressibility is therefore crucial to dynamic stabilization. The shell compression acts as a spring so that the acceleration seen in the Rayleigh-Taylor unstable region actually changes sign even though the laser beam pushes the shell only inward. For dynamic stabilization to work, an average destabilizing acceleration must at least change sign and the oscillating component must exceed appreciably the constant component in amplitude.

In pellet fusion schemes where the implosion requires electron, ion or heavy ion beams to provide the energy required at the pellet surface, the ablation layer, and potentially R-T unstable region beneath, nevertheless act as a spring storing up compressional energy. If the impinging particle beam were interrupted or reduced in intensity, the stored compressional energy is again available to provide a reverse acceleration just as in the case of a modulated laser. Thus dynamic stabilization is potentially useful for these charged-particle-beam fusion schemes as well. A shaped cavity could be used to modulate relativistic electron beams[5] and similar electromagnetic or magnetic techniques during the formation, acceleration and transport of ion beams might readily be employed. The beams could be played back and forth across the pellet surface, for example. In all these cases, based on our laser–D-T shell calculations, modulation frequencies of a few tenths to a few cycles per nanosecond seem to be required. This would demand particle bunches from 15 to 60 cm in length. For large charged-particle-driven systems one might expect modulations even slower than one cycle per nanosecond to be effective because the sonic response time of a thicker ablation layer would be correspondingly slower.

The theory and calculations presented in this paper support the suggestion that an appreciable band of the unstable Rayleigh-Taylor spectrum on the surface of an imploding laser pellet can be stabilized by modulating the intensity of the driving laser beams. By just stabilizing the linearly most unstable mode, the band of stabilization can be made to extend to modes with wavelengths more than 10 times the shell thickness. The growth of longer wavelength modes may not be stabilized by the modulation but the implosion time is sufficiently short that these residual modes should not have time to seriously distort the shell before implosion occurs.

Acknowledgments

The author wishes to thank Steve Bodner and Wally Manheimer for many useful discussions. The author also wishes to thank Professor J. A. Wheeler for demonstrating dynamic stabilization of an inverted pendulum in a freshman physics lecture many years ago. This work was supported by the Office of Naval Research.

JAY P. BORIS

Plasma Physics Division,
Naval Research Laboratory,
Washington, D.C., 20375

References

1. R. E. Kidder, Nuclear Fusion **16**, (1) (1976).
2. G. Zimmerman, Lawrence Livermore Laboratory Report U.C.R.L.–74811, also J. D. Lindl, and W. C. Mead, Lawrence Livermore Laboratory Report U.C.R.L.–77041, Oct. 1975.
3. J. Boris, *Proceedings of the Second European Conference on Computational Physics*, (Garching, 27–30 April 1976), North-Holland. For basic algorithms and splitting techniques see J. P. Boris and D. L. Book, Chapter 3, *Methods in Computational Physics, Vol. 16*, (Academic Press, New York, 1976) and J. P. Boris, U.S. Naval Research Laboratory Memorandum Report 3237, March 1976.
4. M. Abramowitz and I. Stegun, eds., *Handbook of Mathematical Functions*, AMS-55, GPO-June 1964. Also P. M. Morse and H. Feshbach, *Methods of Theoretical Physics, Vol. I*, Chapter 5, (McGraw-Hill, New York, 1953).
5. M. Friedman (private communication).